Structure-Aided Optimization of Kinase Inhibitors Derived from Alsterpaullone

Conrad Kunick,*[a] Zhihong Zeng,[b] Rick Gussio,[c] Daniel Zaharevitz,[c] Maryse Leost,[d] Frank Totzke,[e] Christoph Schächtele,[e] Michael H. G. Kubbutat,[e] Laurent Meijer,[d] and Thomas Lemcke[b]

*In order to perform computer-aided design of novel alsterpaullone derivatives, the vicinity of the entrance to the ATP-binding site was scanned for areas that could be useful as anchoring points for additional protein–ligand interactions. Based on the alignment of alsterpaullone in a CDK1/cyclin B homology model, substituents were attached to the 2-position of the parent scaffold to enable contacts within the identified areas. Synthesis of the designed structures revealed three derivatives (**3**–**5**) with kinase-inhibitory activity similar to alsterpaullone. The novel 2-cyanoethylalsterpaullone (**7**) proved to be the most potent paullone described so far, exhibiting inhibitory concentrations for CDK1/cyclin B and GSK-3β in the picomolar range.*

Introduction

Protein kinases play a fundamental role in manifold physiological events in living organisms, enabling cross talk between cells and constituting a major mechanism of intracellular signaling pathways. The importance of protein phosphorylation is reflected by the fact that 518 putative protein kinase genes have been identified in the human genome.[1] Abnormal protein phosphorylation is observed in diseases like cancer or Alzheimer's disease (AD).[2,3] Consequently, it appears rewarding to look for selective and potent kinase inhibitors, not only with a view to developing new drugs but also to generating tools for investigation of the pathobiochemical role of kinases in diseases. Over the past decade, numerous classes of small synthetic kinase inhibitors have been developed that compete with ATP for binding in the ATP-binding pocket and show greater or lesser selectivity for distinct kinases or kinase families.[4] Among the established kinase-inhibitor classes are the paullones with the lead structure kenpaullone (**1**).

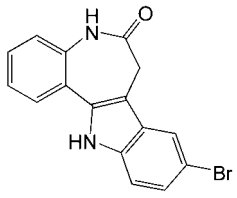

1

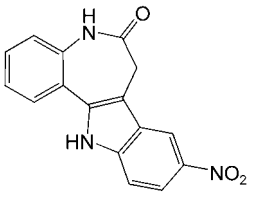

2

Kenpaullone was originally identified from the NCI database of compounds tested in the antitumor drug screen (NCI-ADS) in the course of our program directed at finding novel inhibitors of cyclin-dependent kinases (CDKs).[5] CDKs are a family of serine/threonine kinases that regulate the cell cycle, apoptosis, neuronal-cell physiology, and transcription. Because hyperactivity of CDKs has been detected in many human tumors and cultured tumor cell lines, inhibition of this kinase family has been proposed as a rational approach to fighting cancer diseases,[6] and several structural families of CDK inhibitors have been developed to this end.[7,8] The structure modification of kenpaullone led to alsterpaullone (**2**), which proved to be ten times more active a CDK inhibitor and a hundred times more active an antiproliferative agent than kenpaullone.[9]

For further investigations exploring the intracellular molecular targets, matrix-bound paullones were employed in protein-affinity purification experiments, which confirmed glycogen synthase kinase-3α and β (GSK-3α and β) as additional proteins with paullone affinity.[10,11] GSK-3 is an enzyme involved in diverse multiple processes, including glucose metabolism, dorsoventral patterning during development, Wnt signaling, cell-cycle regulation, and microtubule stabilization.[12–14] Both GSK-3 isoforms proved to be inhibited by nanomolar concentrations of alsterpaullone. Hence, paullones constitute a family of dual CDK/GSK3 inhibitors, a kinase selectivity pattern that is also found with members of the indirubin[15] and aloisine[16] kinase-inhibitor families and with hymenialdisine.[17] In a recently pub-

[a] *Prof. C. Kunick*
Institut für Pharmazeutische Chemie, Technische Universität Braunschweig
Beethovenstraße 55, 38106 Braunschweig (Germany)
Fax: (+49) 531-391-2799
E-mail: c.kunick@tu-bs.de

[b] *Dr. Z. Zeng, Dr. T. Lemcke*
Institut für Pharmazie, Universität Hamburg
Bundesstraße 45, 20146 Hamburg (Germany)

[c] *Dr. R. Gussio, Dr. D. Zaharevitz*
Developmental Therapeutics Program
Division of Cancer Treatment and Diagnosis, National Cancer Institute
Rockville, Maryland 20852 (USA)

[d] *M. Leost, Prof. L. Meijer*
Centre National de la Recherche Scientifique, Station Biologique
B.P. 74, 29682 Roscoff (France)

[e] *Dr. F. Totzke, Dr. C. Schächtele, Dr. M. H. G. Kubbutat*
ProQinase GmbH
Breisacher Straße 117, 79106 Freiburg (Germany)

 DOI: 10.1002/cbic.200400099

lished comparison of commercially available kinase inhibitors, the combined use of kenpaullone and roscovitine was suggested for identifying the substrates and biological roles of CDKs, while kenpaullone and lithium chloride were proposed for exploring the function of GSK-3 in biochemical models.[18] Considerable interest has been devoted to the fact that the paullones inhibit both CDK5 and GSK-3, because both enzymes are involved in the phosphorylation of the microtubule-stabilizing protein tau. In its hyperphosphorylated form, tau constitutes the main part of neurofibrillary tangles that are observed as aggregates in the brain cells of patients suffering from AD.[19,20] In sf9 cells expressing human tau 23 protein, alsterpaullone significantly suppressed tau phosphorylation at AD-characteristic epitopes.[10] Furthermore, alsterpaullone was used to demonstrate the role of phosphorylated tau for organelle transport in differentiated cells. Upon GSK-3 inhibition by alsterpaullone, mitochondrial clustering was observed in association with tau phosphorylation.[21] Most interestingly, paullones are also able to interfere with the generation of the amyloid-β (Aβ) peptide, the main constituent of extracellular amyloid plaques in the brains of AD patients. In a recent paper, Phiel and co-workers showed that kenpaullone significantly decreases the Aβ production in CHO-APP_{695} cells.[22] Hence, the paullones might have the potential for the development of therapeutics to inhibit both the formation of extracellular plaques and intracellular neurofibrillary tangles in AD.

Considering the findings with paullones in AD-related test systems, it is of evident interest to develop further paullones with enhanced activity. With a view to enabling a structure-guided design, we have generated a CoMSIA model for the inhibition of CDK1/cyclin B by paullones, based on a docked alignment of 52 paullones in a CDK1 homology model.[23] Furthermore, the inhibitor alignment was also used for the generation of CoMSIA models for CDK5 and GSK-3 inhibition, albeit the predictive ability for the two latter enzymes was inferior compared to CDK1.[24] The alignment used for the CoMSIA model construction allows a subtle inspection of interactions between inhibitor and CDK1 protein within and in the near vicinity of the ATP-binding pocket. We report here upon the structure-guided design, synthesis, and biological evaluation of novel alsterpaullone derivatives leading to a very potent paullone exhibiting kinase inhibitory activity in the picomolar range.

Results and Discussion

Design of novel alsterpaullone derivatives

In the model of alsterpaullone docked into the ATP-binding site of the CDK1 homology model, the ligand is held in position by a double hydrogen-bonding system to the hinge area in the kinase connecting the N- and the C-terminal domain. This hydrogen bonding involves the lactam carbonyl group of the paullone and the Leu83 nitrogen on the one hand and the paullone lactam nitrogen and the Leu83 carbonyl group on the other. This same hydrogen bonding pattern to amino acids in the hinge area is characteristic of many other kinase inhibitors.[25] The paullone parent scaffold of the condensed benzazepine and indolo ring system is sandwiched between a hydrophobic area composed of the side chains of Ile10/Val18 on the top and the side chain of Leu134 at the bottom of the ATP-binding cleft. The hydrogen bonding between the indole nitrogen of the inhibitor and one of the side-chain oxygen atoms of Asp86 is typical for paullones (Figure 1). Additionally, the 9-nitro substituent of alsterpaullone may form hydrogen bonds with water molecules in the vicinity of Lys33 and Asp145, which are available to serve as ambident nucleophiles for hydrolysis of ATP phosphodiester bonds. This includes a water molecule that was found to interact with the aromatic π cloud of Phe80 in the CDK2 crystal structure.

In order to design novel alsterpaullone derivatives with enhanced potency, we inspected the vicinity of the entrance to the ATP-binding cleft with regard to the alsterpaullone alignment. We speculated that, in the entrance region, the addition of substituents to the alsterpaullone basic structure would be tolerated without disrupting its binding mode. Three main subregions of interest were located:

A) A hydrophobic area composed of the hydrocarbon side chains of Ile10 (A1) and Leu298/Met85 (A2),
B) A salt bridge between the Lys89 amino group and the Asp86 carboxyl group, and
C) A salt bridge formed by three amino acids: the terminal carboxyl function of Gln300, the ω amino group of Lys20, and the side-chain carboxyl function of Glu8 (Figure 2).

To target areas B or C, aliphatic side chains were added at the 2-position of alsterpaullone, and polar substituents were placed at a distance of two or three methylene units to

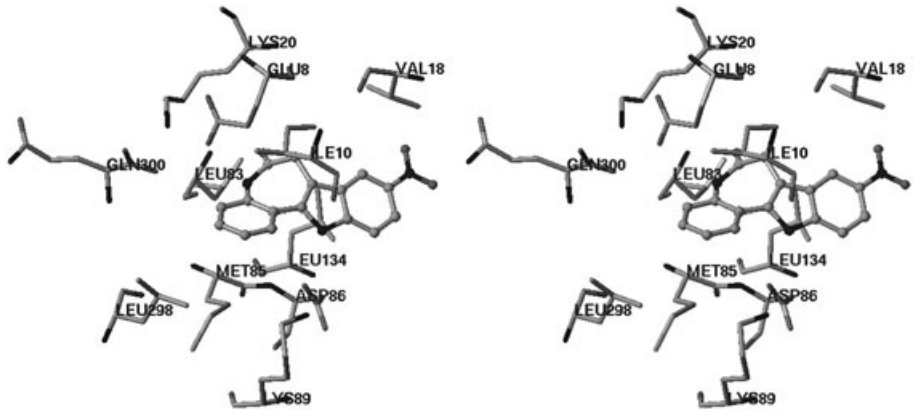

Figure 1. *Stereoview of alsterpaullone docked into the ATP-binding site of the CDK1 homology model. The ligand is depicted in the ball and stick layout, while amino acid portions of CDK1 are given in stick mode.*

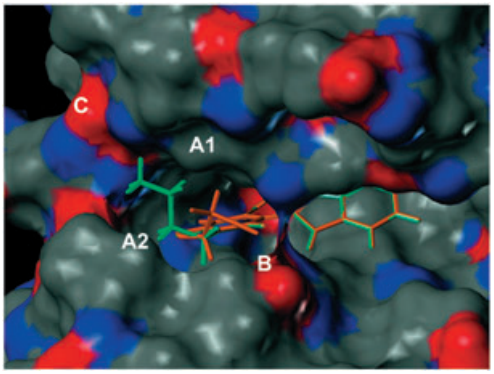

Figure 2. *2-Aminobutylalsterpaullone (**3**, green) and 2-cyanoethylalsterpaullone (**7**, orange) aligned in the ATP-binding pocket of the CDK1 homology model. H-donor positions are red and H-acceptor positions are blue. The hydrocarbon side chains of Ile10 and Leu298 form hydrophobic regions above (A1) and below (A2) the pocket entrance, respectively. B indicates a salt bridge between the protonated amino group of Lys89 (red) and the Asp86 carboxylate group (blue). The blue structure coalescing stalactite-like with area B is the carbonyl oxygen of Ile10. C is a salt-bridge-fixed element consisting of the terminal carboxyl function of Gln300 (blue), the protonated amino group of Lys20 (red), and the side-chain carboxyl function of Glu8 (blue). The protonated amino group of **3** interacts via a salt bridge or hydrogen bond with area C (see also Figure 3). The cyano group of 2-cyanoethylalsterpaullone (**7**) is directed toward the protonated side-chain nitrogen of Lys89 (area B) forming an additional hydrogen bond and enabling hydrophobic contacts between the carbons of the ethylene bridge of **7** and areas A1 (methyl group of Ile10) and A2 (side chains of Leu298 and Met85). See also Figure 4.*

the alsterpaullone ring system. By following this layout, five derivatives were designed: 2-aminobutylalsterpaullone (**3**), 2-aminopropylalsterpaullone (**4**), alsterpaullone-2-propionic acid (**5**), alsterpaullone-2-propionic acid methyl ester (**6**), and 2-cyanoethylalsterpaullone (**7**). Although the potential anchoring points B and C are located in a solvent-exposed area of the kinase, and therefore polar interactions at these motifs might not add a high contribution to the binding affinity, the geometry of the described binding mode would enable hydrophobic contacts between the areas A1/2 and the aliphatic linker chains. It was envisaged that these hydrophobic contacts would especially lead to increased binding affinity and consequently enhanced kinase inhibition by **3**–**7**.

For the generation of binding models, the molecules were manually docked into the ATP-binding cleft of the CDK1 homology model and subsequently energy minimized by using the program suite MOLOC with the implemented MAB force field.[26,27] The side chains in the 2-position were adjusted manually to enable contacts either with area C (**3** and **4**), or with area B (**5**–**7**), and energy minimization was repeated. The resulting side-chain conformations are shown in Figures 2–4. In Figure 2, the conformations of **3** and **7** are depicted. From this image it becomes obvious that the protonated amino group of **3** can easily interact through a salt bridge or hydrogen bond with area C (see also Figure 3). The cyano group of **7** is directed toward the protonated side-chain nitrogen of Lys89 (area B) forming an additional hydrogen bond (see also Figure 4) enabling hydrophobic contacts between the carbons of the ethylene bridge of **7** and areas A1 (methyl group of Ile10) and A2 (side chains of Leu298 and Met85).

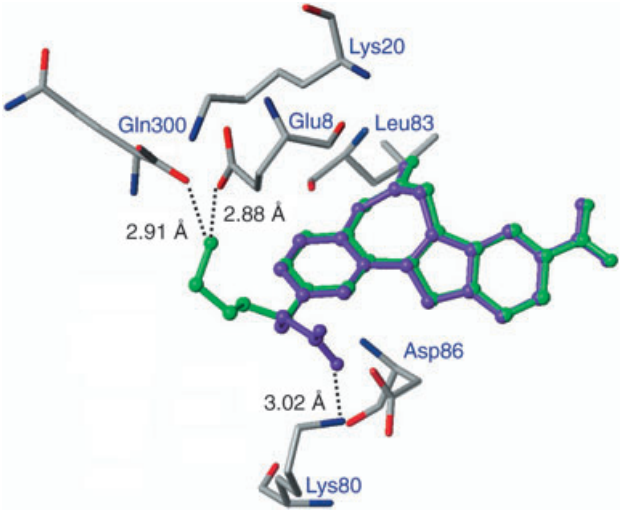

Figure 3. *2-Aminobutylalsterpaullone (**3**, green) and alsterpaullone-3-propionic acid (**5**, violet) in the ATP-binding cleft of the CDK1 homology model. Dotted lines represent putative hydrogen bonds. The protonated amino group of **3** is directed toward the salt bridge triad motif formed by the C-terminal Gln300, Lys20, and Glu8. The carboxylate group of **5** is directed toward the protonated amino group of the Lys89 side chain, which itself interacts with the Asp86 carboxylate group through a salt bridge.*

Chemistry

A Heck reaction[28] was employed for the introduction of side chains into the 2-position of the paullones. For this coupling reaction, an iodo substituent in the 2-position of the paullone scaffold is favorable.[29] Because attempts to prepare 2-iodo-9-nitropaullone by a Fischer indole reaction were not successful, the introduction of side chains by Heck reaction was performed before the indolization reaction was performed. For this purpose, the general key compound 7-iodo-1*H*-[1]benzazepine-2,5(3*H*,4*H*)-dione (**8**) was treated with terminal alkenes.[29] Upon treatment of **8** with *N*-3-butenylphthalimide (**9**)

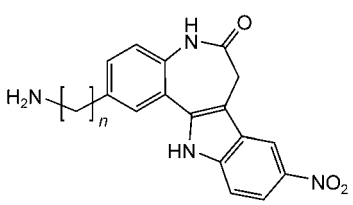

3 (*n* = 4)
4 (*n* = 3)

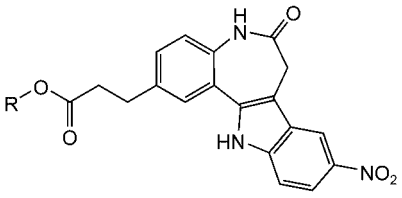

5 (R = H)
6 (R = CH_3)

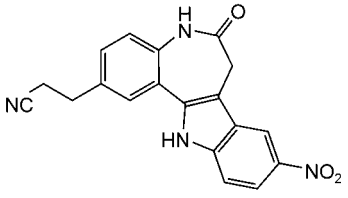

7

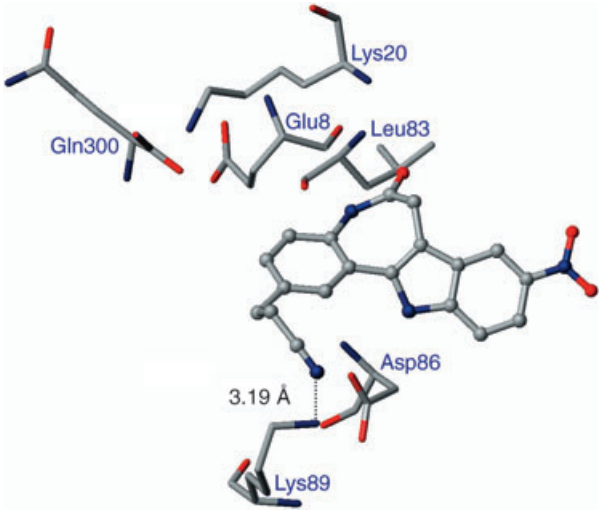

Figure 4. *2-Cyanoethylalsterpaullone (**7**) in the ATP-binding cleft of the CDK1 homology model. The cyano nitrogen lone pair points toward the protonated amino group of the Lys89 side chain, forming a hydrogen bond.*

in the presence of 5 mol% $Pd(OAc)_2$ and 10 mol% PPh_3 as catalysts in DMF, the alkene **10** was obtained in moderate yield as a mixture of *E*/*Z* diastereomers (Scheme 1). Subsequently, the alkene double bond was easily saturated by hydrogenation over 10% Pd/C in ethanol. The intermediate **11** thus prepared was treated with 4-nitrophenylhydrazine in glacial acetic acid, and the resulting nitrophenylhydrazone **12** was cyclized by means of a thermal Fischer indole reaction in refluxing diphenyl ether to furnish the paullone **13**. The phthalimido group was then cleaved by hydrazinolysis in boiling ethanol to yield the desired amino compound **3**.

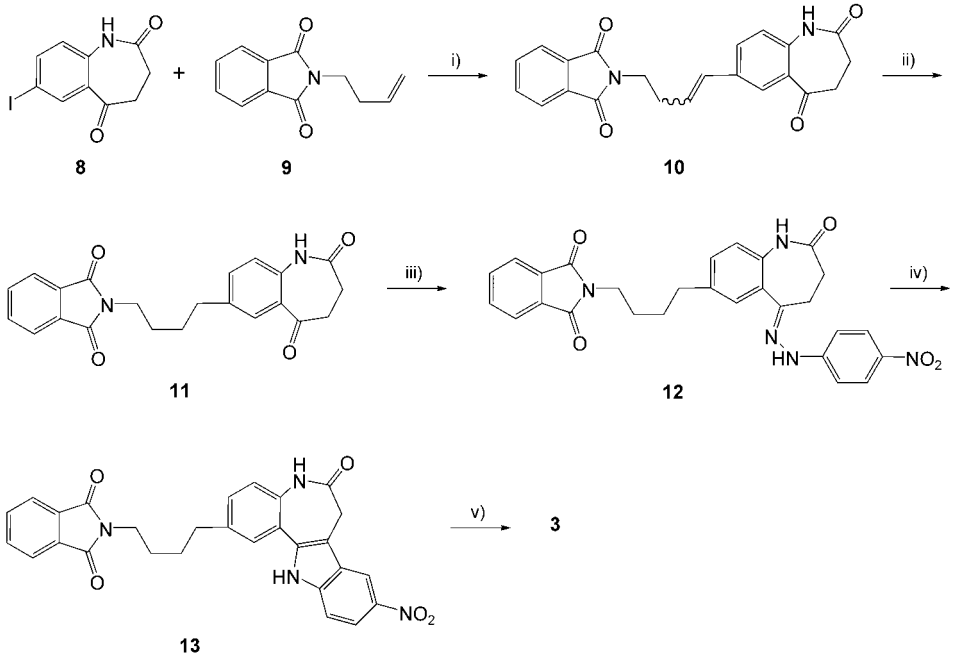

Scheme 1. *Reagents and conditions: i) $Pd(OAc)_2$, Et_3N, PPh_3, DMF, 100°C (48%); ii) Pd/C, 2 atm H_2, 6 h, RT (92%); iii) 4-nitrophenylhydrazine, HOAc, 70°C (50%); iv) diphenyl ether, reflux, N_2 (55%); v) hydrazine, ethanol, reflux (50%).*

2-Aminopropyl-alsterpaullone (**4**) was synthesized by using a similar approach, which is outlined in Scheme 2. In this sequence, the *N*-allylphthalimide **14** was employed in the Heck reaction leading to the alkene intermediate **15**. As a result of the very poor solubility of **15** in common organic solvents, it was not possible to employ a catalytic hydrogenation procedure for the saturation of the alkene double bond. Therefore, **15** was treated with 4-nitrophenylhydrazine to yield the phenylhydrazone **16**. The ring closure leading to the paullone **17** was then accomplished by heating **16** under reflux in diphenyl ether. Eventually, prolonged heating of **17** with hydrazine hydrate in ethanol in air concomitantly led to hydrogenation of the alkene double bond and cleavage of the phthalimido group in a one-pot reaction. Under the reaction conditions used in this step, hydrazine is air-oxidized to give diimide, which serves as the actual reducing agent for the carbon–carbon double bond.[30] The important advantage of this method over catalytic hydrogenation lies in the selectivity of the diimide, which does not reduce the nitro group under the conditions employed.

For the synthesis of the alsterpaullone propionic acid derivatives **5**, **6**, and **7**, the sequence starts with a Heck reaction of the central intermediate **8** and acrylonitrile (**18**) or acrylic acid methyl ester (**19**). Catalytic hydrogenation of the double bond of **20**/**21**, conversion of the intermediates **22**/**23** to the 4-nitrophenylhydrazones **24** and **25**, and subsequent indole formation led to the new paullones **6** and **7**. Hydrolysis of **6** with sodium hydroxide in a dioxane/water mixture furnished the desired carboxylic acid **5** (Scheme 3).

Biological evaluation and discussion

Biological evaluation revealed that the five novel alsterpaullone derivatives **3**–**7** are potent inhibitors of the kinases CDK1/cyclin B, CDK5/p25, and GSK-3β. A closer look at the test results given in Table 1 shows that **3**–**5** inhibit the three kinases in the same order of magnitude as alsterpaullone. Hence, in these cases the introduction of the side chains was tolerated but failed to enhance the kinase inhibitory activity. However, derivatives **3**–**5** are able to form water-soluble salts, a feature that in biochemical test systems constitutes a main advantage over the poorly water soluble alsterpaullone. Compared to the carboxylic acid **5**, the corresponding methyl ester **6** is roughly four times less active a kinase inhibitor. This fact can be explained with a steric interaction of the ester methyl group

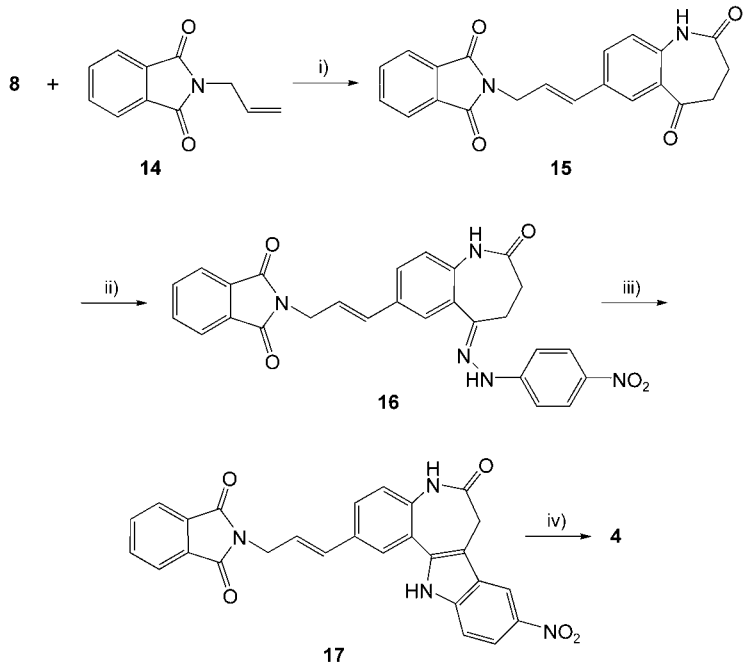

Scheme 2. *Reagents and conditions: i) $Pd(OAc)_2$, Et_3N, PPh_3, DMF, 100 °C (62 %); ii) 4-nitrophenylhydrazine, HOAc, 70 °C (82 %); iii) diphenyl ether, reflux, N_2 (70 %); iv) hydrazine, ethanol, air, reflux (40 %).*

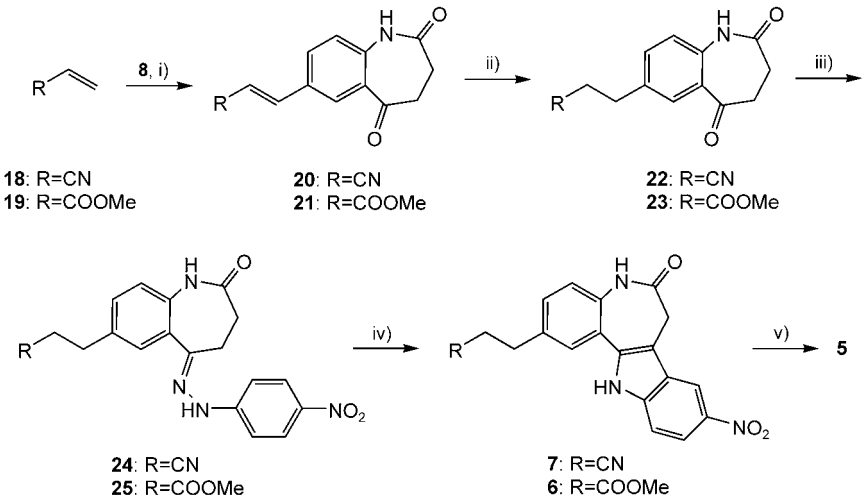

Scheme 3. *Reagents and conditions: i) $Pd(OAc)_2$, Et_3N, PPh_3, DMF, 80 °C (68 %/79 %); ii) Pd/C, 2 atm H_2, 6 h, RT (74 %/89 %); iii) 4-nitrophenylhydrazine, HOAc, 70 °C (53 %/75 %); iv) diphenyl ether, reflux, N_2 (56 %/72 %); v) 1. NaOH, dioxane, H_2O, RT; 2. HCl (54 %).*

and the Ile10 carbonyl function (the "stalactite" structure in the entrance to the ATP binding cleft as depicted in Figure 2), if similar binding modes are assumed for **5** and **6** (see Figure 3 for binding mode of **5**). The cyanoethyl-substituted alsterpaullone derivative **7** exhibited a very potent kinase inhibitory activity, namely on CDK1/cyclin B and on GSK-3β. With respect to the noteworthy differences in potency between 2-cyanoethyl-alsterpaullone **7** and the other novel alsterpaullone derivatives **3**–**6**, the suggested binding mode based on our model does not deliver a completely satisfactory explanation. If, on the one hand, the increase in potency found with **7** is actually caused by the additional contacts as depicted in Figure 4, the other structures **3**–**6** should similarly exhibit a higher activity compared to the unsubstituted alsterpaullone. If, on the other hand, the binding mode model constructed for **3**–**6** is correct, the corresponding model for **7** would fail to explain the remarkable increase in activity observed for this derivative.

A comparison of the inhibitory activity data predicted by our CoMSIA models with the experimental data shows that the structural modification at the 2-position of paullones is not satisfactorily described. While the CDK1 inhibition of **3**, **4**, and **6** and the CDK5 inhibition of **3**, **4** and **7** are sufficiently predicted (residuals of $pIC_{50} < 0.5$), the GSK-3β inhibition is generally underpredicted. Similarly, major deviations are found for two CDK1 predictions (compounds **5** and **7**) and two CDK5 predictions (compounds **5** and **6**). Given that the CoMSIA model had efficiently predicted the kinase inhibitory activity of a test set of 23 paullones that did not bear sterically demanding substituents in the 2-position, the latter structural modification is apparently not reflected in the CoMSIA model. There are two possible reasons for this drawback. First, the model was constructed on the basis of a training set of 52 compounds, of which only six were 2-substituted with chains comprising more than three atoms in a row.[24] Furthermore, these chains were not manually manipulated before energy minimization, and hence the model is not able to correctly handle the conformations we have constructed and displayed in Figures 2, 3 and 4. Second, the CoMSIA models were constructed by using a docked alignment in a CDK1 homology model. This alignment was then used for the building of the CDK5 and the GSK-3β models. That means, in the vicinity of the ATP-binding-site entrance of both CDK5 and GSK-3β, major differences are found compared to the architecture of CDK1, and consequently the predictive power of the model for 2-substituted compounds is low for CDK5 and GSK-3β. Given the high relevance of GSK-3 inhibitors in the search for therapeutics against Alzheimer's disease, we will carry out design studies in the future on the basis of the recently published crystal-structure data of the alsterpaullone/GSK-3β-complex.[31]

As mentioned above, the ATP-binding site of protein kinases is a highly conserved area. Given the large number of kinases

Table 1. *Determined and predicted kinase inhibitory properties of the alsterpaullone derivatives 2-7.*[a]

Paullone	IC_{50} [nM]			pIC_{50} [M]					
	GSK-3β	CDK1/cyclin B	CDK5/p25	GSK-3β observed	GSK-3β predicted	CDK1/cyclin observed	CDK1/cyclin B predicted	CDK5/p25 observed	CDK5/p25 predicted
2[b]	4	35	40	8.40	n.a.[c]	7.46	n.a.[c]	7.40	n.a.[c]
3	6	80	70	8.22	6.86	7.10	7.13	7.16	7.19
4	2.5	27	23	8.60	7.31	7.57	7.25	7.64	7.34
5	6.5	25	80	8.19	6.5	7.60	6.85	7.10	6.40
6	34	100	250	7.47	7.22	7.00	7.23	6.60	7.39
7	0.8	0.23	30	9.10	7.21	9.64	7.35	7.52	7.32

[a] Standard errors of the IC_{50} values are typically below 20%. In many cases, standard errors below 10% are found. [b] Values taken from ref. [10]. [c] Not applicable.

that interfere with manifold biochemical processes in living organisms, the selectivity for distinct kinases is a major issue for novel developed inhibitors. In order to check the selectivity of the novel potent dual GSK-3/CDK-inhibitor **7**, the compound was profiled in the commercially available testing screen of the ProQinase Company (Freiburg, Germany) by determining the IC_{50} values against 20 kinases. The test panel comprised serine/threonine kinases and tyrosine kinases, among them membrane-located receptor kinases and cytoplasmic enzymes. The profiling results showed that **7** indeed preferentially inhibited serine/threonine kinases from the CDK/GSK-3 family. However, some receptor tyrosine kinases (VEGFR-2 and VEGFR-3) and Src are also inhibited in the submicromolar range. In consequence, the selectivity issue has to be considered in the further development of the paullones as kinase inhibitors. In this regard, the difference of the GSK-3 IC_{50} value for compound **7** found in the automated custom assay (Figure 5) on the one hand and the corresponding value found in the assay carried out manually (Table 1) is striking. A possible explanation is that the recombinant GSK-3β preparations used contain variable proportions of badly folded proteins that are kinase inactive but still bind, and thus trap, the paullones, thereby artificially increasing the IC_{50} values. The observation of this discrepancy constitutes another instructive example for the general conclusion that IC_{50} values from different assays should not be compared directly.[32]

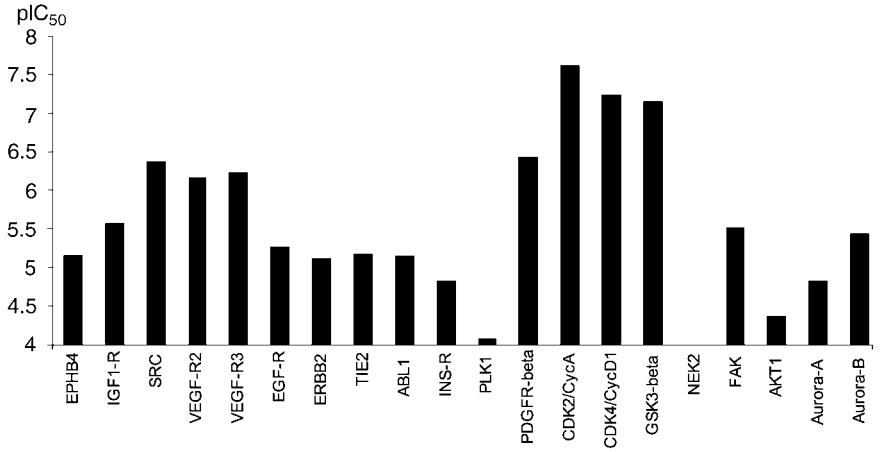

Figure 5. *Results of a custom kinase profiling of compound **7** in an automated assay. $pIC_{50} = -\log IC_{50}$ [M].*

Experimental Section

Melting points (m.p.) were determined on an electric variable heater (Electrothermal 9100) and are uncorrected. Elemental analyses were performed in the analytical department of the Institut für Pharmazie, Universität Hamburg. Column chromatography was performed by using chromatography-grade silica gel 60 (Merck). NMR spectra were recorded on a Bruker AMX 400 instrument, by using tetramethylsilane as internal standard and [D_6]dimethylsulfoxide as solvent unless stated otherwise. High-resolution FAB mass spectra (HRMS) were determined on a Finnigan MAT 311A instrument with 3-nitrobenzyl alcohol as matrix.

(*E*)-7-(4-Phthalimidobut-1-en-1-yl)-1*H*-[1]benzazepine-2,5(3*H*,4*H*)-dione (10): A solution of 7-iodo-1*H*-[1]benzazepine-2,5(3*H*,4*H*)-dione (**8**)[29] (440 mg, 1.5 mmol), triethylamine (1.0 mL), *N*-(but-3-enyl)phthalimide (**9**) (400 mg, 2.0 mmol), palladium acetate (10 mg, 0.045 mmol), and triphenylphosphine (20 mg, 0.09 mmol) in DMF (20 mL) was heated to 100 °C under nitrogen for 6 h. After cooling, the mixture was poured into water (80 mL). The precipitate was filtered by suction, washed with hexane, and purified by column chromatography (silica gel, toluene/acetone 3:1), to give 260 mg (48%) of a slightly yellow powder. M.p. 217 °C; ^{1}H NMR: $\delta = 10.06$ (s, 1H), 7.84 (m, 4H), 7.70 (d, $J = 2.2$ Hz, 1H), 7.55 (dd, $J = 2.2$, 8.3 Hz, 1H), 7.09 (d, $J = 8.3$ Hz, 1H), 6.43 (d, $J = 16.0$ Hz, 1H), 6.23 (dt, $J = 6.9$, 16.0 Hz, 1H), 3.73 (t, $J = 6.9$ Hz, 2H), 2.89 (m, 2H), 2.65 (m, 2H), 2.51 (m, 2H); IR: 3200, 1760, 1700, 1660, 1480, 1380, 1210, 1180, 710 cm^{-1}; elemental analysis calcd (%) for ($C_{22}H_{18}N_2O_4$): C 70.58, H 4.85, N 7.48; found: C 69.91, H 4.83, N 7.28.

7-(4-Phthalimidobutyl)-1*H*-[1]benzazepine-2,5(3*H*,4*H*)-dione (11): 10% Pd/C (50 mg) was added to a solution of 7-(4-phthalimidobuten-1-yl)-1*H*-[1]benzazepine-2,5(3*H*,4*H*)-dione (**10**; 225 mg, 0.6 mmol) in ethanol (200 mL). The mixture was hydrogenated at 2 atm for 6 h. Subsequently, the catalyst was filtered off and washed with ethanol. The combined filtrate was evaporated to give the crude product, which was purified by column chromatography on silica gel (toluene/acetone 3:1) to give 210 mg (92%) of a white solid. M.p. 221 °C; ^{1}H NMR: $\delta = 9.98$ (s, 1H), 7.84 (m, 4H), 7.61 (d, $J = 2.3$ Hz, 1H), 7.38 (dd, $J = 2.3$, 8.1 Hz, 1H), 7.06 (d, $J = 8.1$ Hz, 1H), 3.59 (t, $J = 6.6$ Hz, 2H), 2.87 (m, 2H), 2.63 (m, 2H), 2.59 (t, 2H, $J = 6.9$ Hz), 1.58 (m, 4H).

7-(4-Phthalimidobutyl)-5-(4-nitrophenylhydrazono)-4,5-dihydro-1*H*-[1]benzazepin-2(3*H*)-one (12): A slurry of 7-(4-phthalimidobutyl)-1*H*-[1]benzazepine-2,5(3*H*,4*H*)-dione (**11**; 150 mg, 0.4 mmol) and 4-nitrophenylhydrazine (100 mg, 0.65 mmol) in acetic acid (3 mL) was heated to 70 °C for 3 h. After being cooled to RT, the mixture was poured into 5% Na_2CO_3 solution (10 mL). The precipitate was

filtered by suction, washed with water, and crystallized from ethanol to give 103 mg (50%) of an orange solid. M.p. 250°C (dec.); ^{1}H NMR: δ = 10.09 (s, 1H), 9.67 (s, 1H), 8.11 (d, J = 9.1 Hz, 2H), 7.83 (m, 4H), 7.45 (d, J = 1.8 Hz, 1H), 7.30 (d, J = 9.1 Hz, 2H), 7.19 (dd, J = 1.8, 8.1 Hz, 1H), 6.93 (d, J = 8.1 Hz, 1H), 3.63 (t, J = 6.6 Hz, 2H), 3.03 ("t", J = 6.5 Hz, 2H), 2.63 (t, J = 7.3 Hz, 2H), 2.53 ("t", J = 6.5 Hz, 2H), 1.64 (m, 4H).

2-(4-Phthalimidobutyl)-9-nitro-7,12-dihydroindolo[3,2-*d*][1]benzazepin-6(5*H*)-one (13): 7-(4-Phthalimidobutyl)-5-(4-nitrophenylhydrazono)-4,5-dihydro-1*H*-[1]benzazepin-2(3*H*)-one (**12**; 200 mg, 0.39 mmol) was suspended in diphenyl ether (20 mL). The mixture was heated under reflux for 2 h under nitrogen, and then cooled to RT. Upon addition of petroleum ether (40 mL) a solid was formed, which was filtered with suction, washed with petroleum ether, and crystallized from ethanol to give 106 mg (55%) of a brown powder. M.p. > 300°C; ^{1}H NMR: δ = 12.32 (s, 1H), 10.10 (s, 1H), 8.72 (d, J = 2.3 Hz, 1H), 8.07 (dd, J = 2.3, 8.9 Hz, 1H), 7.85 (m, 4H), 7.60 (d, J = 2.2 Hz, 1H), 7.59 (d, J = 8.9 Hz, 1H), 7.28 (dd, J = 2.2, 8.4 Hz, 1H), 7.18 (d, J = 8.4 Hz, 1H), 3.64 (m, 2H), 3.63 (s, 2H), 2.69 (m, 2H), 1.68 (m, 4H).

2-(4-Aminobutyl)-9-nitro-7,12-dihydroindolo[3,2-*d*][1]benzazepin-6(5*H*)-one hydrochloride (3HCl): Hydrazinium hydroxide (1 mL) was added to a suspension of 2-(4-phthalimidobutyl)-9-nitro-7,12-dihydroindolo[3,2-*d*][1]benzazepin-6(5*H*)-one (**13**; 322 mg, 0.65 mmol) in ethanol (50 mL). The mixture was heated under reflux for 6 h. After cooling, the solvent was evaporated under reduced pressure. The residue was rinsed with NaOH solution (1 N, 20 mL). A solid formed that was separated by centrifugation and washed with water (3×20 mL). The solid was then added to water (100 mL) and concentrated hydrochloride acid (0.1 mL). The resulting mixture was heated to 60°C for 30 min. After filtering off the insoluble solid, the filtrate was concentrated in vacuo to give 130 mg (50%) of a brown powder. M.p. > 300°C; ^{1}H NMR: δ = 12.48 (s, 1H), 10.15 (s, 1H), 8.73 (d, J = 2.3 Hz, 1H), 8.08 (dd, J = 2.3, 8.9 Hz, 1H), 7.77 (br s, 3H), 7.65 (d, J = 1.5 Hz, 1H), 7.61 (d, J = 8.9 Hz, 1H), 7.29 (dd, J = 1.5, 8.4 Hz, 1H), 7.21 (d, J = 8.4 Hz, 1H), 3.62 (s, 2H), 2.82 (m, 2H), 2.68 (m, 2H), 1.72 (m, 2H), 1.60 (m, 2H); elemental analysis calcd (%) for $C_{20}H_{21}N_4O_3Cl{\cdot}1.5\,H_2O$: C 54.99, H 5.76, N 12.82; found: C 54.42, H 5.66, N 13.01; HRMS (FAB, $C_{20}H_{20}N_4O_3$): calcd: 365.1614, found: 365.1596.

7-(3-Phthalimidopropen-1-yl)-1*H*-[1]benzazepine-2,5(3*H*,4*H*)-dione (15): Synthesized as described for compound **10**, with **8**[29] (450 mg, 1.5 mmol), triethylamine (1.0 mL), *N*-(prop-2-enyl)phthalimide (**14**; 400 mg, 2.1 mmol), palladium acetate (10 mg, 0.045 mmol), and triphenylphosphine (20 mg, 0.09 mmol) in DMF (20 mL). Crystallized from dichloromethane to yield 337 mg (62%) of a slightly yellow powder. M.p. > 270°C (dec.); ^{1}H NMR: δ = 10.10 (s, 1H), 7.84 (m, 4H), 7.79 (d, J = 2.0 Hz, 1H), 7.65 (dd, J = 2.0, 8.4 Hz, 1H), 7.10 (d, J = 8.4 Hz, 1H), 6.59 (d, J = 16.0 Hz, 1H), 6.30 (dt, J = 5.6, 16.0 Hz, 1H), 4.36 (dd, J = 1.0, 5.6 Hz, 2H), 2.89 (m, 2H), 2.65 (m, 2H).

7-(3-Phthalimidopropen-1-yl)-5-(4-nitrophenylhydrazono)-4,5-dihydro-1*H*-[1]benzazepin-2(3*H*)-one (16): Synthesized according to the method described for **12**, with **15** (200 mg, 0.56 mmol) and 4-nitrophenylhydrazine (200 mg, 1.3 mmol) in acetic acid (5 mL). Crystallized from ethanol to give 227 mg (82%) of orange solid. M.p. 307°C (dec.); ^{1}H NMR: δ = 10.11 (s, 1H), 9.78 (s, 1H), 8.13 (d, J = 9.1 Hz, 2H), 7.86 (m, 4H), 7.61 (d, J = 2.0 Hz, 1H), 7.47 (dd, J = 2.0, 8.4 Hz, 1H), 7.31 (d, J = 9.1 Hz, 2H), 6.97 (d, J = 8.4 Hz, 1H), 6.63 (d, J = 15.8 Hz, 1H), 6.31 (dt, J = 15.8, 5.8 Hz, 1H), 4.37 (d, J = 5.8 Hz, 2H), 3.04 ("t", J = 6.5 Hz, 2H), 2.54 ("t", J = 6.5 Hz, 2H).

2-(3-Phthalimidopropen-1-yl)-9-nitro-7,12-dihydroindolo[3,2-*d*][1]benzazepin-6(5*H*)-one (17): Synthesized as described for **13**, with **16** (150 mg, 0.30 mmol) in diphenyl ether (15 mL). Crystallized from ethanol to give 102 mg (70%) of a brown powder. M.p. > 310°C; ^{1}H NMR: δ = 12.33 (s, 1H), 10.21 (s, 1H), 8.72 (d, J = 2.0 Hz, 1H), 8.06 (dd, J = 2.0, 8.9 Hz, 1H), 7.90 (m, 4H), 7.80 (d, J = 1.6 Hz, 1H), 7.56 (d, J = 8.9 Hz, 1H), 7.52 (dd, J = 1.6, 8.4 Hz, 1H), 7.22 (d, J = 8.4 Hz, 1H), 6.62 (d, J = 15.5 Hz, 1H), 6.41 (dt, J = 15.5, 5.7 Hz, 1H), 4.41 (d, J = 5.7 Hz, 2H), 3.64 (s, 2H).

2-(3-Aminopropyl)-9-nitro-7,12-dihydroindolo[3,2-*d*][1]benzazepin-6(5*H*)-one hydrochloride (4HCl): Hydrazinium hydroxide (1 mL) was added to a suspension of 2-(phthalimidoprop-4-en-1-yl)-9-nitro-7,12-dihydroindolo[3,2-*d*][1]benzazepin-6(5*H*)-one (**17**; 214 mg, 0.45 mmol) in ethanol (20 mL). Subsequently, the mixture was heated under reflux for 24 h in the presence of air. After cooling, the solvent was evaporated under reduced pressure. The residue was rinsed with NaOH solution (1 N, 20 mL), the formed fine solid was separated by centrifugation and washed with water (3× 20 mL). The solid was then added to water (100 mL) and concentrated hydrochloride acid (0.1 mL). The resulting mixture was heated to 60°C for 30 min, the insoluble solid was filtered off, and the filtrate was concentrated to give 70 mg (40%) of a brown powder. M.p. > 300°C; ^{1}H NMR: δ = 12.54 (s, 1H), 10.17 (s, 1H), 8.74 (d, J = 2.0 Hz, 1H), 8.08 (dd, J = 2.0, 9.2 Hz, 1H), 7.90 (br s, 3H), 7.66 (d, J = 1.8 Hz, 1H), 7.62 (d, J = 8.9 Hz, 1H), 7.30 (dd, J = 1.8, 8.4 Hz, 1H), 7.22 (d, J = 8.1 Hz, 1H), 3.63 (s, 2H), 2.83 (m, 2H), 2.72 (t, J = 7.5 Hz, 2H), 1.95 (m, 2H); elemental analysis calcd (%) for $C_{19}H_{19}N_4O_3Cl{\cdot}H_2O$: C 56.37, H 5.23, N 13.84; found: C 55.97, H 5.06, N 13.23; HRMS: calcd: 350.1377 $[C_{19}H_{18}N_4O_3]^+$, found: 350.1369; calcd: 351.1457 $[C_{19}H_{18}N_4O_3{+}H]^+$, found: 351.1453.

3-(2,5-Dioxo-2,3,4,5-tetrahydro-1*H*-[1]benzazepin-7-yl)-acrylonitrile (20): Synthesized as described for compound **10**, with **8** (448 mg, 1.5 mmol), triethylamine (1.0 mL), acrylonitrile (**18**; 1.10 mL, 15 mmol), palladium acetate (19 mg, 0.09 mmol), and triphenylphosphine (43 mg, 0.17 mmol) in DMF (20 mL), reaction time 2 h. Purified by column chromatography (petroleum ether/ethyl acetate 1:1) to yield 230 mg (68%) of a mixture of *E*/*Z* products as slightly yellow powder. ^{1}H NMR: (*Z* form): δ = 10.42 (s, 1H), 8.39 (d, J = 2.3 Hz, 1H), 8.04 (dd, J = 2.28, 8.4 Hz, 1H), 7.49 (d, J = 11.9 Hz, 1H), 7.34 (d, J = 8.4 Hz, 1H), 5.92 (d, J = 11.9 Hz, 1H), 3.00 (m, 2H), 2.78 (m, 2H). (*E* form): δ = 10.37 (s, 1H), 8.11 (d, J = 2.0 Hz, 1H), 7.93 (dd, J = 2.04, 8.4 Hz, 1H), 7.75 (d, J = 16.8 Hz, 1H), 7.28 (d, J = 8.4 Hz, 1H), 6.49 (d, J = 16.8 Hz, 1H), 3.01 (m, 2H), 2.77 (m, 2H); elemental analysis calcd (%) for $C_{13}H_{10}N_2O_2$: C 69.02, H 4.45, N 12.38; found: C 69.01, H 4.65, N 11.23.

3-(2,5-Dioxo-2,3,4,5-tetrahydro-1*H*-[1]benzazepin-7-yl)-propionitrile (22): Synthesized according to the method described for **11**, with **20** (160 mg, 0.7 mmol), ethanol (200 mL), and 10% Pd/C (50 mg). Purified by column chromatography (petrol ether/ethyl acetate 1:1) to give 120 mg (74%) white solid. M.p. 198°C; ^{1}H NMR: δ = 10.05 (s, 1H), 7.74 (d, J = 2.3 Hz, 1H), 7.48 (dd, J = 2.3, 8.4 Hz, 1H), 7.13 (d, J = 8.4 Hz, 1H), 2.93–2.86 (m, 4H), 2.80 (m, 2H), 2.65 (m, 2H); elemental analysis calcd (%) for $C_{13}H_{12}N_2O_2$: C 68.41, H 5.30, N 12.27; found: C 68.37, H 5.40, N 11.91.

3-(2-Oxo-5-(4-nitrophenylhydrazono)-2,3,4,5-tetrahydro-1*H*-[1]benzazepin-7-yl)-propionitrile (24): Synthesized according to the method described for **12** with **22** (110 mg, 0.48 mmol), acetic acid (4 mL), and 4-nitrophenylhydrazine (115 mg, 0.75 mmol). Recrystallization from ethanol gave 92 mg (53%) of an orange solid. M.p. > 285°C (dec.); ^{1}H NMR: δ = 10.13 (s, 1H), 9.74 (s, 1H), 8.12 (d, J = 9.2 Hz, 2H), 7.60 (d, J = 2.0 Hz, 1H), 7.36 (d, J = 9.2 Hz, 2H), 7.29

(dd, $J=2.0$, 8.2 Hz, 1H), 6.99 (d, $J=8.2$ Hz, 1H), 3.05 ("t", $J=6.6$ Hz, 2H), 2.92 (m, 2H), 2.84 (m, 2H), 2.55 ("t", $J=6.6$ Hz, 2H).

3-(6-Oxo-9-nitro-5,6,7,12-tetrahydroindolo[3,2-*d*][1]benzazepin-2-yl)propionitrile (7): Synthesized as described for **13** with **24** (58 mg, 0.16 mmol) in diphenyl ether (5 mL). Recrystallization from ethanol gave 40 mg (72%) of a brown powder. M.p. > 300 °C; ^{1}H NMR: $\delta=12.35$ (s, 1H), 10.17 (s, 1H), 8.73 (d, $J=2.3$ Hz, 1H), 8.08 (dd, $J=2.3$, 8.9 Hz, 1H), 7.69 (d, $J=1.8$ Hz, 1H), 7.61 (d, $J=8.9$ Hz, 1H), 7.38 (dd, $J=1.8$, 8.1 Hz, 1H), 7.24 (d, $J=8.1$ Hz, 1H), 3.65 (s, 2H), 2.97 (m, 2H), 2.90 (m, 2H); HRMS (FAB) calcd: 346.1065 $[C_{19}H_{14}N_4O_3]^+$; found: 346.1080, calcd: 347.1144 $[C_{19}H_{14}N_4O_3+H]^+$, found: 347.1157.

(*E*)-3-(2,5-Dioxo-2,3,4,5-tetrahydro-1*H*-[1]benzazepin-7-yl)prop-2-enonic acid methyl ester (21): Synthesized as described for compound **10** with **8** (800 mg, 2.66 mmol), triethylamine (1.0 mL), prop-2-enonic acid methyl ester (**19**; 1.10 mL, 15 mmol), palladium acetate (20 mg, 0.1 mmol), and triphenylphosphine (40 mg, 0.15 mmol) in DMF (15 mL); reaction temperature 80 °C. Recrystallization from ethanol gave 542 mg (79%) of a slightly yellow powder. M.p. > 240 °C (dec.); ^{1}H NMR: $\delta=10.30$ (s, 1H), 8.06 (d, $J=2.0$ Hz, 1H), 7.96 (dd, $J=2.0$, 8.4 Hz, 1H), 7.67 (d, $J=16.0$ Hz, 1H), 7.21 (d, $J=8.4$ Hz, 1H), 6.60 (d, $J=16.0$ Hz, 1H), 3.72 (s, 3H), 2.93 (m, 2H), 2.70 (m, 2H).

3-(2,5-Dioxo-2,3,4,5-tetrahydro-1*H*-[1]benzazepin-7-yl)-propionic acid methyl ester (23): Synthesized according to the method described for **11**, employing **21** (450 mg, 1.7 mmol), THF (200 mL), and 10% Pd/C (50 mg). Purification by column chromatography (petroleum ether/ethyl acetate 1:1) gave 400 mg (89%) of a white solid. M.p. 145 °C; ^{1}H NMR: $\delta=10.02$ (s, 1H), 7.65 (d, $J=2.0$ Hz, 1H), 7.42 (dd, $J=2.0$, 8.4 Hz, 1H), 7.08 (d, $J=8.4$ Hz, 1H), 3.58 (s, 3H), 2.89 (m, 2H), 2.84 (t, $J=7.6$ Hz, 2H), 2.64 (m, 2H), 2.62 (t, $J=7.6$ Hz, 2H); elemental analysis calcd (%) for $C_{14}H_{15}NO_4$: C 64.36, H 5.79, N 5.36; found: C 64.45, H 5.78, N 5.35.

3-(2-Oxo-5-(4-nitrophenylhydrazono)-2,3,4,5-tetrahydro-1*H*-[1]benzazepin-7-yl)-propionic acid methyl ester (25): Synthesized according to the method described for **12** with **23** (300 mg, 1.15 mmol), glacial acetic acid (5 mL), and 4-nitrophenylhydrazine (300 mg, 2.0 mmol). Crystallization from methanol yielded 340 mg (75%) of an orange solid. M.p. > 260 °C (dec.); ^{1}H NMR: $\delta=10.13$ (s, 1H), 9.71 (s, 1H), 8.14 (d, $J=9.4$ Hz, 2H), 7.50 (d, $J=2.0$ Hz, 1H), 7.33 (d, $J=9.4$ Hz, 2H), 7.23 (dd, $J=2.0$, 8.1 Hz, 1H), 6.95 (d, $J=8.1$ Hz, 1H), 3.61 (s, 3H), 3.04 (t, $J=6.3$ Hz, 2H), 2.88 (t, $J=7.5$ Hz, 2H), 2.67 (t, $J=7.5$ Hz, 2H), 2.53 (t, $J=6.3$ Hz, 2H); elemental analysis calcd (%) for $C_{20}H_{20}N_4O_5$: C 60.60, H 5.09, N 14.13; found: C 60.22, H 4.94, N 14.12.

3-(6-Oxo-9-nitro-5,6,7,12-tetrahydroindolo[3,2-*d*][1]benzazepin-2-yl)propionic acid methyl ester (6): Synthesized as described for **13** with **25** (280 mg, 0.71 mmol) in diphenyl ether (20 mL). Crystallization from methanol gave 150 mg (56%) of a brown powder. M.p. > 300 °C; ^{1}H NMR: $\delta=12.35$ (s, 1H), 10.14 (s, 1H), 8.73 (d, $J=2.0$ Hz, 1H), 8.07 (dd, $J=2.0$, 8.9 Hz, 1H), 7.64 (d, $J=1.5$ Hz, 1H), 7.60 (d, $J=8.9$ Hz, 1H), 7.31 (dd, $J=1.5$, 8.4 Hz, 1H), 7.20 (d, $J=8.4$ Hz, 1H), 3.63 (s, 2H), 3.61 (s, 3H), 2.94 (t, $J=7.6$ Hz, 2H), 2.73 (t, $J=7.6$ Hz, 2H); HRMS calcd: 379.1166 $[C_{20}H_{17}N_3O_5]^+$, found: 379.1201, calcd: 380.1246 $[C_{20}H_{17}N_3O_5+H]^+$, found: 380.1255.

3-(6-Oxo-9-nitro-5,6,7,12-tetrahydroindolo[3,2-*d*][1]benzazepin-2-yl)propionic acid (5): Sodium hydroxide solution (1 M, 2 mL) was added to a solution of 3-(6-oxo-9-nitro-5,6,7,12-tetrahydroindolo[3,2-*d*][1]benzazepin-2-yl)propionic acid methyl ester (**6**; 200 mg, 0.53 mmol) in 1,4-dioxane (5 mL). The mixture was stirred at RT for 4 h. Subsequently, the mixture was cooled to 0 °C, and concentrated hydrochloric acid (0.2 mL) was added dropwise. A solid precipitated, which was filtered off, washed with water (3×10 mL), and crystallized from ethanol to give 104 mg (54%) of a yellow powder. M.p. > 300 °C; ^{1}H NMR: $\delta=12.36$ (s, 1H), 12.18 (br s, 1H), 10.13 (s, 1H), 8.72 (d, $J=2.0$ Hz, 1H), 8.07 (dd, $J=2.0$, 8.9 Hz, 1H), 7.64 (d, $J=1.8$ Hz, 1H), 7.60 (d, $J=8.9$ Hz, 1H), 7.31 (dd, $J=2.0$, 8.3 Hz, 1H), 7.19 (d, $J=8.3$ Hz, 1H), 3.63 (s, 2H), 2.90 (t, $J=7.6$ Hz, 2H), 2.63 (t, $J=7.6$ Hz, 2H); elemental analysis calcd (%) for $C_{19}H_{15}N_3O_5\cdot1.5\,H_2O$: C 58.16, H 4.62, N 10.71; found: C 58.44, H 4.44, N 10.68.

Kinase assays

Reagents: Homogenization buffer: β-glycerophosphate (60 mM), *p*-nitrophenylphosphate (15 mM), Mops (25 mM; pH 7.2), ethyleneglycol bis(2-aminoethylether)tetraacetic acid (EGTA; 15 mM), $MgCl_2$ (15 mM), dithiothreitol (DTT, 1 mM), sodium vanadate (1 mM), NaF (1 mM), phenylphosphate (1 mM), leupeptin (10 μg mL^{-1}), aprotinin (10 μg mL^{-1}), soybean trypsin inhibitor (10 μg mL^{-1}), and benzamidine (100 μg). Buffer A: $MgCl_2$ (10 mM), EGTA (1 mM), DTT (1 mM), Tris/HCl (25 mM; pH 7.5), heparin (50 μg mL^{-1}). Buffer C: homogenization buffer but with 5 mM EGTA, no NaF, and no protease inhibitors. Kinase activities were assayed in duplicates in buffer A or C at 30 °C and at a final ATP concentration of 15 μM. The order of mixing the reagents was: buffers, substrate, enzyme, inhibitor. There was no preincubation at 30 °C. Addition of radiolabeled ATP was considered as time $t=0$ of the incubation period. Assays were run under conditions in which less than 5% of the radiolabeled phosphate was incorporated. Blank values were subtracted, and activities were calculated as pmol of phosphate incorporated for a 10 min incubation. The activities are usually expressed in percentage of the maximal activity, that is, in the absence of inhibitors. Controls were performed with appropriate dilutions of DMSO.

GSK-3β: GSK-3β was expressed in and purified from insect Sf9 cells.[33] It was assayed, following a 1:100 dilution in 1 mg bovine serum albumin per mL 10 mM DTT, with GS-1 peptide (5 μL 40 μM) as a substrate, in buffer A, in the presence of [γ-^{32}P]ATP (15 μM, 3000 Ci mmol^{-1}, 1 mCi mL^{-1}) in a final volume of 30 μL. After 30 min incubation at 30 °C, 25 μL aliquots of supernatant were spotted onto 2.5×3 cm pieces of Whatman P81 phosphocellulose paper, and, 20 s later, the filters were washed five times (for at least 5 min each time) in a solution of phosphoric acid (10 mL per liter of water). The wet filters were counted in the presence of ACS (1 mL, Amersham) scintillation fluid.

CDK1/cyclin B. CDK1/cyclin B was extracted in homogenization buffer from M-phase starfish (*Marthasterias glacialis*) oocytes and purified by affinity chromatography on p9^{CKShs1} Sepharose beads, from which it was eluted by free p9^{CKShs1} as previously described.[34] The kinase activity was assayed in buffer C, with histone H1 (1 mg mL), in the presence of [γ-^{32}P]ATP (15 μM, 3000 Ci mmol^{-1}, 1 mCi mL^{-1}) in a final volume of 30 μL. After 10 min incubation at 30 °C, 25 μL aliquots of supernatant were spotted onto P81 phosphocellulose papers and treated as described above.

CDK5/p25. CDK5/p25 was reconstituted by mixing equal amounts of recombinant mammalian CDK5 and p25 expressed in *E. coli* as GST (glutathione S-transferase) fusion proteins and purified by affinity chromatography on glutathione–agarose (vectors kindly provided by J. H. Wang, Department of Medical Chemistry, University of Calgary, Alberta, Canada; p25 is a truncated version of the p35, the 35 kDa CDK5 activator). Its activity was assayed in buffer C as described for CDK1/cyclin B.

Custom kinase inhibition assays for Ins-R, PDGF-Rb, CDK4/D1, Aurora A, Aurora BCDK2/AAKT1, IGF1-R, SRC, VEGF-R2, EGF-R, EPHB4, ErbB2, FAK, TIE2, VEGF-R3, PLK1, GSK3β, NEK2, Abl: The assays were performed in an automated system run by the ProQinase Company (Freiburg, Germany). All protein kinases were expressed in Sf9 insect cells as human recombinant GST-fusion proteins or His-tagged proteins by means of the baculovirus expression system. Kinases were purified by affinity chromatography by using either GSH–agarose (Sigma) or Ni-NTH–agarose (Qiagen). The purity and identity of each kinase was checked by SDS-PAGE/silver staining and by Western blotting analysis with specific antibodies. A proprietary protein kinase assay (33 PanQinase® Activity Assay) was used for measuring the kinase activity of the 20 protein kinases. All kinase assays were performed in 96-well FlashPlates™ from Perkin Elmer/NEN (Boston, MA, USA) in a 50 μL reaction volume. The reaction cocktail was pipetted in four steps in the following

- 20 μL of assay buffer (standard buffer)
- 5 μL of ATP solution (in H_2O)
- 5 μL of test compound (in 10% DMSO)
- 10 μL of substrate/10 μL of enzyme solution (premixed)

The assay for all enzymes contained HEPES/NaOH (60 mM, pH 7.5), $MgCl_2$ (3 mM), $MnCl_2$ (3 mM), Na-orthovanadate (3 μM), DTT (1.2 mM), PEG20000 (50 μg mL^{-1}), [γ-^{33}P]-ATP (1 μM, ca. 5×10^5 cpm per well).

The reaction cocktails were incubated at 30 °C for 80 min. The reaction was stopped with H_3PO_4 (50 μL, 2% (*v*/*v*)), plates were aspirated and washed twice with H_2O (200 μL) or NaCl (200 μL, 0.9% (*w*/*v*)). Incorporation of $^{33}P_i$ was determined with a microplate scintillation counter (Microbeta, Wallac). All assays were performed with a BeckmanCoulter/Sagian robotic system. With the residual activities (in %) obtained for each concentration, the compound IC_{50} values were calculated by using Prism 3.03 for Windows (Graphpad, San Diego, California, USA; www.graphpad.com). The model used was "Sigmoidal response (variable slope)" with parameters "top" fixed at 100% and "bottom" at 0%.

Acknowledgements

We are grateful to Dr. Ven Narayanan (National Cancer Institute) for support in organizing this project. Funding of the project by the National Cancer Institute (to C.K. and Z.Z.) is gratefully acknowledged. This research was also supported by the European Commission (Contract No LSHB-CT-2004-503467, to C.K., M.H.G.K., and L.M.) and by grants from the "Association pour la Recherche sur le Cancer" (L.M.) and by a grant ("Molécules & Cibles Thérapeutiques") from the "Ministère de la Recherche/ INSERM/CNRS" (L.M.).

Keywords: enzymes · inhibitors · lactams · molecular modeling · paullones · proteins

[1] G. Manning, D. B. Whyte, R. Martinez, T. Hunter, S. Sudarsanam, *Science* **2002**, *298*, 1912 – 1934.
[2] P. Cohen, *Eur. J. Biochem.* **2001**, *268*, 5001 – 5010.
[3] P. Cohen, *Nat. Rev. Drug Discovery* **2002**, *1*, 309 – 315.
[4] C. García-Echeverría, P. Traxler, D. B. Evans, *Med. Res. Rev.* **2000**, *20*, 28 – 57.
[5] D. W. Zaharevitz, R. Gussio, M. Leost, A. Senderowicz, T. Lahusen, C. Kunick, L. Meijer, E. A. Sausville, *Cancer Res.* **1999**, *59*, 2566 – 2569.
[6] M. Knockaert, P. Greengard, L. Meijer, *Trends Pharmacol. Sci.* **2002**, *23*, 417 – 425.
[7] A. Huwe, R. Mazitschek, A. Giannis, *Angew. Chem.* **2003**, *115*, 2170 – 2187; *Angew. Chem. Int. Ed.* **2003**, *42*, 2122 – 2138.
[8] P. M. Fischer, A. Gianella-Borradori, *Expert Opin. Invest. Drugs* **2003**, *12*, 955 – 970.
[9] C. Schultz, A. Link, M. Leost, D. W. Zaharevitz, R. Gussio, E. A. Sausville, L. Meijer, C. Kunick, *J. Med. Chem.* **1999**, *42*, 2909 – 2919.
[10] M. Leost, C. Schultz, A. Link, Y.-Z. Wu, J. Biernat, E.-M. Mandelkow, J. A. Bibb, G. L. Snyder, P. Greengard, D. W. Zaharevitz, R. Gussio, A. M. Senderowicz, E. A. Sausville, C. Kunick, L. Meijer, *Eur. J. Biochem.* **2000**, *267*, 5983 – 5994.
[11] M. Knockaert, K. Wieking, S. Schmitt, M. Leost, K. M. Grant, J. C. Mottram, C. Kunick, L. Meijer, *J. Biol. Chem.* **2002**, *277*, 25 493 – 25 501.
[12] A. Ali, K. P. Hoeflich, J. R. Woodgett, *Chem. Rev.* **2001**, *101*, 2527 – 2540.
[13] B. W. Doble, J. R. Woodgett, *J. Cell Sci.* **2003**, *116*, 1175 – 1186.
[14] S. Frame, P. Cohen, *Biochem. J.* **2001**, *359*, 1 – 16.
[15] P. Polychronopoulos, P. Magiatis, A. L. Skaltsounis, V. Myrianthopoulos, E. Mikros, A. Tarricone, A. Musacchio, S. M. Roe, L. Pearl, M. Leost, P. Greengard, L. Meijer, *J. Med. Chem.* **2004**, *47*, 935 – 946.
[16] Y. Mettey, M. Gompel, V. Thomas, M. Garnier, M. Leost, I. Ceballos-Picot, M. Noble, J. Endicott, J.-M. Vierfond, L. Meijer, *J. Med. Chem.* **2003**, *46*, 222 – 236.
[17] L. Meijer, A.-M. W. H. Thunissen, A. W. White, M. Garnier, M. Nikolic, L.-H. Tsai, J. Walter, K. E. Cleverley, P. C. Salinas, Y.-Z. Wu, J. Biernat, E. M. Mandelkow, S.-H. Kim, G. R. Pettit, *Chem. Biol.* **2000**, *7*, 51 – 63.
[18] J. Bain, H. McLauchlan, M. Elliott, P. Cohen, *Biochem. J.* **2003**, *371*(1), 199 – 204.
[19] E. M. Mandelkow, E. Mandelkow, *Trends Cell Biol.* **1998**, *8*, 425 – 427.
[20] E. Mandelkow, *Nature* **1999**, *402*, 588 – 589.
[21] Y. Tatebayashi, N. Haque, Y. C. Tung, K. Iqbal, I. Grundke-Iqbal, *J. Cell Sci.* **2004**, 1653 – 1663.
[22] C. J. Phiel, C. A. Wilson, V. M.-Y. Lee, P. S. Klein, *Nature* **2003**, *423*, 435 – 439.
[23] R. Gussio, D. W. Zaharevitz, C. F. McGrath, N. Pattabiraman, G. E. Kellogg, C. Schultz, A. Link, C. Kunick, M. Leost, L. Meijer, E. A. Sausville, *Anti-Cancer Drug Des.* **2000**, *15*, 53 – 66.
[24] C. Kunick, K. Lauenroth, K. Wieking, X. Xie, C. Schultz, R. Gussio, D. Zaharevitz, M. Leost, L. Meijer, A. Weber, F. S. Jorgensen, T. Lemcke, *J. Med. Chem.* **2004**, *47*, 22 – 36.
[25] L. M. Toledo, N. B. Lydon, D. Elbaum, *Curr. Med. Chem.* **1999**, *6*, 775 – 805.
[26] P. Gerber, K. Müller, *J. Comput.-Aided Mol. Des.* **1995**, *9*, 251 – 268.
[27] P. Gerber, *J. Comput.-Aided Mol. Des.* **1998**, *12*, 37 – 51.
[28] M. Larhed, A. Hallberg in *Handbook of Organopalladium Chemistry, Vol.* 1 (Ed.: E. Negishi), Wiley, Hoboken, NJ, **2002**, pp. 1133 – 1178.
[29] C. Kunick, C. Schultz, T. Lemcke, D. W. Zaharevitz, R. Gussio, R. K. Jalluri, E. A. Sausville, M. Leost, L. Meijer, *Bioorg. Med. Chem. Lett.* **2000**, *10*, 567 – 569.
[30] A. Furst, R. C. Berlo, S. Hooton, *Chem. Rev.* **1965**, *65*, 51 – 68.
[31] J. A. Bertrand, S. Thieffine, A. Vulpetti, C. Cristiani, B. Valsasina, S. Knapp, H. M. Kalisz, M. Flocco, *J. Mol. Biol.* **2003**, *333*, 393 – 407.
[32] M. A. Sills, D. Weiss, Q. Pham, R. Schweitzer, X. Wu, J. J. Wu, *J. Biomol. Screening* **2002**, *7*, 191 – 214.
[33] K. Hughes, B. J. Pulverer, P. Theocharous, J. R. Woodgett, *Eur. J. Biochem.* **1992**, *203*, 305 – 311.
[34] A. Borgne, A. C. Ostvold, S. Flament, L. Meijer, *J. Biol. Chem.* **1999**, *274*, 11 977 – 11 986.

Received: April 8, 2004
Revised: September 9, 2004
Published online on February 4, 2005

